

Self-consistent band-gap renormalization GW

Vojtěch Vlček,^{1,*} Roi Baer,^{2,†} Eran Rabani,^{3,4,‡} and Daniel Neuhauser^{1,§}

¹*Department of Chemistry and Biochemistry, University of California, Los Angeles California 90095, U.S.A.*

²*Fritz Haber Center for Molecular Dynamics, Institute of Chemistry,
The Hebrew University of Jerusalem, Jerusalem 91904, Israel*

³*Department of Chemistry, University of California and Materials Science Division,
Lawrence Berkeley National Laboratory, Berkeley, California 94720, USA*

⁴*The Raymond and Beverly Sackler Center for Computational Molecular
and Materials Science, Tel Aviv University, Tel Aviv, Israel 69978*

(Dated: January 10, 2017)

Partially-self-consistent gap-renormalization GW (grGW) is introduced to calculate quasiparticle (QP) energies within the many-body perturbation theory of Hedin. Self-consistency of the Green's function is obtained by renormalization of the band gap, removing the most significant approximation of the single-shot G_0W_0 approach. The formalism is performed as a post-processing step and thus, can be implemented within any GW algorithm which calculates the full frequency-dependent self-energies. Here, the grGW approach is combined with the stochastic GW (sGW) formalism developed in [Phys. Rev. Lett. **113**, 076402 (2014)]. The computational cost and scaling are similar to that of the single-shot sGW. We illustrate the approach for two confined semiconducting systems with open boundary conditions: Silicon nanocrystal (NC) quantum dots (QDs) and 2D planar and bent phosphorene nanoribbons (PNRs).

I. INTRODUCTION

The GW approximation¹ to many-body perturbation theory is often used to describe quasiparticle (QP) excitations in molecules, nanostructures, and bulk materials.^{2–15} The formalism builds on the Dyson equation for the single-particle Green's function (GF) in the frequency domain, $\tilde{G}(\mathbf{r}, \mathbf{r}', \omega)$, given by (we set $\hbar = 1$):

$$\begin{aligned} \tilde{G}(\mathbf{r}, \mathbf{r}', \omega) &= \tilde{G}_0(\mathbf{r}, \mathbf{r}', \omega) + \iint d\mathbf{r}_1 d\mathbf{r}_2 \tilde{G}_0(\mathbf{r}, \mathbf{r}_1, \omega) \\ &\times \tilde{\Sigma}(\mathbf{r}_1, \mathbf{r}_2, \omega) \tilde{G}(\mathbf{r}_2, \mathbf{r}', \omega), \end{aligned} \quad (1)$$

where $\tilde{G}_0(\mathbf{r}, \mathbf{r}', \omega)$ is the single particle GF of the reference system, typically taken from the Kohn-Sham¹⁶ (KS) density function theory (DFT),¹⁷ and $\tilde{\Sigma}(\mathbf{r}_1, \mathbf{r}_2, \omega)$ is the self-energy. The GW approximation replaces the exact self-energy with an approximated form, which in the time domain is given by:

$$\tilde{\Sigma}(\mathbf{r}, \mathbf{r}', \omega) = i \int_{-\infty}^{\infty} \frac{d\omega'}{2\pi} \tilde{G}(\mathbf{r}, \mathbf{r}', \omega + \omega') \tilde{W}(\mathbf{r}, \mathbf{r}', \omega') \quad (2)$$

where $\tilde{W}(\mathbf{r}, \mathbf{r}', \omega)$ is the frequency-dependent screened Coulomb interaction. Solving the above equation requires a self-consistent procedure since both $\tilde{\Sigma}(\mathbf{r}, \mathbf{r}', \omega)$ and $\tilde{W}(\mathbf{r}, \mathbf{r}', \omega)$ depend on $\tilde{G}(\mathbf{r}, \mathbf{r}', \omega)$. The self-consistent solution is computationally demanding^{18,19} and thus, several approximate schemes have been developed over the past decade to reduce the computational effort.

Perhaps the most common GW treatment is based on a non-self-consistent scheme^{20,21} combined with KS-DFT as a starting (reference) point. In this scheme, $\tilde{G}(\mathbf{r}, \mathbf{r}', \omega)$ on the right hand side of Eq. (2) is replaced by the reference GF, $\tilde{G}_0(\mathbf{r}, \mathbf{r}', \omega)$, and $\tilde{W}(\mathbf{r}, \mathbf{r}', \omega)$ is calculated

within the random phase approximation (RPA) or time-dependent DFT (TDDFT) accounting for approximate vertex corrections. Both approximations are referred to as “single-shot” GW. The former is named G_0W_0 and the latter G_0W . The single-shot GW provides significant improvements over the bare KS-DFT results, but often underestimate the QP (fundamental) gaps and the ionization potentials (IP) compared to experiment.^{8,22–27} Moreover, the QP energies depend on the choice of the reference system and fail when the reference system solution of the QP energies is far from the fully many-body picture.

Circumventing the dependence on the reference system requires a fully self-consistent solution of Eqs. (1) and (2).^{10,23,28,29} While computationally more demanding, in principle, a fully self-consistent solution is expected to be more accurate than the single-shot approach, since it accounts for some of the higher order terms in the screened Coulomb interaction. However, in many situations it is less accurate than the single-shot GW for QP energies in comparison to experiments.^{8,30}

An alternative to the fully self-consistent treatment of GW is based on a partially self-consistent approach.^{8,28,30} partially self-consistent GW (pGW) was applied successfully to bulk systems with a small unit cell^{8,30,31} and to organic molecules,^{27–29} resulting in QP energies and fundamental band gaps that are consistently in better agreement with experiment than both the single-shot and the fully self-consistent approaches. However, this comes at a more demanding computational cost compared to G_0W_0 or G_0W , limiting the size of systems that can be described within the pGW method.

In this paper, we develop a new partially self-consistent GW approach, where the GF is solved self-consistently but the screened coulomb interaction is still calculated within the RPA or TDDFT approximations using the

reference point states and energies, similar to the single-shot approach. This allows for a simple renormalization of the band gap, removing the most significant approximation of the single-shot approach. The formalism can be performed as a post-processing step and thus, can easily be implemented within any GW algorithm that generates $\tilde{\Sigma}(\mathbf{r}, \mathbf{r}', \omega)$. In this respect, the approach is highly suitable for a stochastic formulation³²⁻⁴⁰ which produces the self-energy at all frequencies.⁴¹ The stochastic GW (sGW) was applied to study QP energies and IPs in molecules,⁴² polymers,⁴³ and silicon quantum-dot (QD) nanocrystals (NCs),⁴¹ with great success. Yet, since it is based on G_0W_0 or G_0W it suffers from the same inaccuracies as the deterministic version of these approaches, and thus often underestimates the fundamental gaps and ionization potentials.⁴²

Here, we show that these flaws can be corrected using the partially self-consistent gap-renormalization grGW approach. As an example, we revisit the problem of QP energies in silicon QDs and find an increase of the G_0W_0 fundamental gaps by as much as 0.45 eV. We also apply the method to 2D phosphorene nanoribbons (PNRs), where high sensitivity to external perturbations such as bending and stress were found using KS and/or hybrid DFT.⁴⁴⁻⁴⁸ These effects are addressed within the grGW for the first time.

The paper is organized as follows: In Sec. II we outline the grGW method. Results for Si NCs and phosphorene nanoribbons are presented and discussed in Sec. III. Finally, we conclude in Sec. IV.

II. METHOD

The starting point of a GW calculation is a reference system, often taken from a KS-DFT equation, $\hat{h}_{KS}\phi_n^{KS}(\mathbf{r}) = \varepsilon_n^{KS}\phi_n^{KS}(\mathbf{r})$, where the KS Hamiltonian is (from now on we employ atomic units):

$$\hat{h}_{KS} = -\frac{1}{2}\nabla^2 + v_{\text{ext}}(\mathbf{r}) + v_{\text{H}}(\mathbf{r}) + v_{\text{xc}}(\mathbf{r}). \quad (3)$$

Here, $v_{\text{ext}}(\mathbf{r})$, $v_{\text{H}}(\mathbf{r}) = \int n(\mathbf{r}')|\mathbf{r} - \mathbf{r}'|^{-1}d\mathbf{r}'$ and $v_{\text{xc}}(\mathbf{r})$ are the external, Hartree and exchange-correlation potentials respectively. The latter two potential depend on the ground state electron density $n(\mathbf{r}) = 2\sum_n f_n \phi_n^{KS}(\mathbf{r})^2$ where f_n is the KS eigenstate occupation number (1 for occupied and 0 for empty eigenstates). The GW QP energy, ε_n^{QP} , is then expressed as a perturbative correction to the KS energy:^{20,21}

$$\varepsilon_n^{QP} = \varepsilon_n^{KS} + \tilde{\Sigma}_n(\omega) - V_{xc}^n, \quad (4)$$

where $V_{xc}^n = \int v_{xc}(\mathbf{r})|\phi_n^{KS}(\mathbf{r})|^2 d\mathbf{r}$ is the average exchange-correlation potential, and $\tilde{\Sigma}_n(\omega)$ is the expectation value of the GW self-energy at a frequency ω ,

$$\tilde{\Sigma}_n(\omega) = \iint \phi_n^{KS}(\mathbf{r})\tilde{\Sigma}(\mathbf{r}, \mathbf{r}', \omega)\phi_n^{KS}(\mathbf{r}')d\mathbf{r}d\mathbf{r}'. \quad (5)$$

The GW self-energy, $\tilde{\Sigma}(\mathbf{r}, \mathbf{r}', \omega)$, is given in terms of a convolution integral in the frequency domain (see Eq. (2)), which can be expressed as a product in the time domain ($\Sigma(\mathbf{r}, \mathbf{r}', t) = \int_{-\infty}^{\infty} \tilde{\Sigma}(\mathbf{r}, \mathbf{r}', \omega) e^{-i\omega t} \frac{d\omega}{2\pi}$):

$$\Sigma(\mathbf{r}, \mathbf{r}', t) = G(\mathbf{r}, \mathbf{r}', t)W(\mathbf{r}, \mathbf{r}', t^+). \quad (6)$$

Here, $W(\mathbf{r}, \mathbf{r}', t)$ is obtained from an RPA ($W_0(\mathbf{r}, \mathbf{r}', t)$) or TDDFT calculation (see Ref. 42 for further details) and $G(\mathbf{r}, \mathbf{r}', t)$ is the partially self-consistent GF:

$$iG(\mathbf{r}, \mathbf{r}', t) = \text{tr} \left\{ |\mathbf{r}\rangle \langle \mathbf{r}'| e^{-i(\hat{h}_{KS} + \hat{\Delta})t} \left[\theta(t)\theta_{\beta}(\hat{h}_{KS} - \mu) - \theta(-t)\theta_{\beta}(\mu - \hat{h}_{KS}) \right] \right\}, \quad (7)$$

where we approximate the correction to the KS Hamiltonian as $\hat{\Delta} = \sum_n |\phi_n^{KS}\rangle \Delta_n \langle \phi_n^{KS}|$ i.e. an operator diagonal in the KS basis and $\Delta_n = \varepsilon_n^{QP} - \varepsilon_n^{KS}$ is the QP shift of level n .

To obtain the QP energies within the pGW, one requires as input the self-energy evaluated at ε_n^{QP} . In the single-shot GW, this is the only condition in Eq. (4) to achieve a self-consistent solution. In the pGW, the self-energy depends on ε_n^{QP} also through $\hat{\Delta}$ and thus, one is required to recalculate $\tilde{\Sigma}_n(\omega)$ from Eqs. (5)-(7) for each self-consistent iteration.

A significant simplification is achieved by recognizing that $\Delta_{n \leq n_{\text{Fermi}}} \approx \Delta_v$ and $\Delta_{n > n_{\text{Fermi}}} \approx \Delta_c$, independent of the band index n . Namely, that the QP shift is similar for all occupied states (Δ_v) and for all unoccupied states (Δ_c). Thus, one can simplify Eq. (7) and remove the dependence on the KS orbitals:

$$iG(\mathbf{r}, \mathbf{r}', t) = \text{tr} \left\{ |\mathbf{r}\rangle \langle \mathbf{r}'| e^{-i\hat{h}_{KS}t} \left[\theta(t) e^{-i\Delta_c t} \theta_{\beta}(\hat{h}_{KS} - \mu) - \theta(-t) e^{-i\Delta_v t} \theta_{\beta}(\mu - \hat{h}_{KS}) \right] \right\}. \quad (8)$$

We see that the partially self-consistency approximation we suggest involves multiplying the GF by a time-dependent phase factor $e^{-i\Delta(t)}$ where $\Delta(t) = \theta(-t)\Delta_v + \theta(t)\Delta_c$. This translates directly to a simple correction of the self-energy, $\Sigma_n(t)$, in the time domain:

$$\Sigma_n(t) = \Sigma_n^{(0)}(t) e^{-i\Delta(t)t}, \quad (9)$$

where $\Sigma_n^{(0)}(t)$ is the G_0W_0 or G_0W self-energy obtained using the GF in Eq. (8) with $\Delta(t) = 0$.

The partially self-consistent GW approach is summarized as follows:

1. Generate the G_0W_0 or G_0W self-energy, $\tilde{\Sigma}_n^{(0)}(\omega)$, for KS eigenstate n . Set $\tilde{\Sigma}_n(\omega) = \tilde{\Sigma}_n^{(0)}(\omega)$.
2. Solve Eq. (4) for ε_n^{QP} and obtain $\Delta_n = \varepsilon_n^{QP} - \varepsilon_n^{KS}$ for the valance band maximum (VBM, Δ_v) and conduction band minimum (CBM, Δ_c) orbitals.

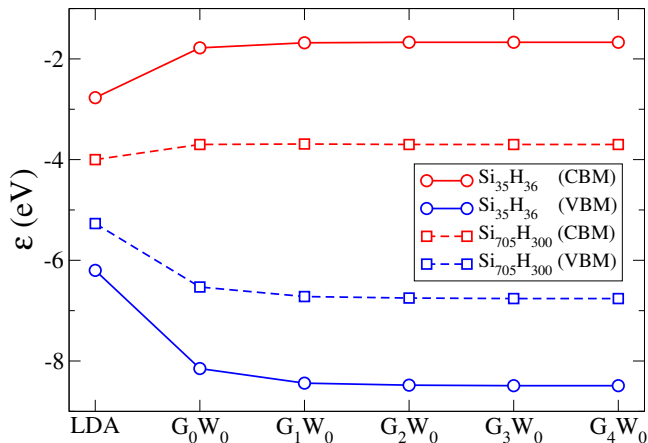


Figure 1. QP energies of the conduction band minimum (CBM) and valance band maximum (VBM) of $\text{Si}_{35}\text{H}_{36}$ and $\text{Si}_{705}\text{H}_{300}$ (with 176 and 3120 valence electrons). The LDA starting point of the calculation is also shown for reference. The partially self-consistent sGW iterations are labeled as $G_0W_0 \cdots G_4W_0$.

3. Generate $\Sigma_n(t)$ from Eq. (9) and use Fourier transform to generate $\tilde{\Sigma}_n(\omega) = \int_{-\infty}^{\infty} \Sigma_n(t) e^{i\omega t - \gamma|t|} dt$, where γ is a small regularization parameter.
4. Repeat step (2) and (3) until convergence.

The pGW approach herewith delineated is a post-processing step which is applicable to any G_0W_0 approximation which produces the self energy in time or frequency space. We illustrate the method in the next section using the sGW approach, developed in Ref. 41. For completeness we give a brief summary of sGW in Appendix A. The resulting method is then dubbed sgrGW.

III. RESULTS

A. Silicon NC QDs

We first apply sgrGW for calculating the VBM and CBM QP energies for two silicon QDs: $\text{Si}_{35}\text{H}_{36}$ and $\text{Si}_{705}\text{H}_{300}$, with 176 and 3120 valence electrons, respectively. The QD geometry is taken from bulk silicon with experimental lattice constant of 5.43\AA , with atoms three dangling bonds are removed from the structure and hydrogen atoms are used for passivation of the surface.⁴⁹

We have performed LDA calculations within a real-space grid approach using the Troullier-Martins pseudopotentials.⁵⁰ We used a grid of size 64^3 and $\hbar = 0.5a_0$ for $\text{Si}_{35}\text{H}_{36}$, and 108^3 grid points with $\hbar = 0.6a_0$ for $\text{Si}_{705}\text{H}_{300}$. The LDA density, VBM and CBM were used as inputs for the sgrGW calculations with $N_\zeta = 10000$ and 1400 for the small and large QD, respectively, and $N_\xi = 100$ and $N_\eta = 8$ for both systems. The time-grid for $\Sigma_n(t)$ and all other time-dependent quantities spanned the range $[-T, T]$ where $T = 100\hbar E_h^{-1}$ and the time step

was $\Delta t = 0.05\hbar E_h^{-1}$ and the regularization parameter was $\gamma = 0.04\hbar^{-1} E_h$.

In Fig. 1 we show the CBM and VBM LDA and sgrGW QP energies for the two silicon QDs as a function of the self-consistent iterations. For both QDs, the VBM (CBM) energy decreases (increases) and rapidly converges. The first iteration (single-shot sGW, labeled as G_0W_0) changes the VBM (CBM) by a sizable amount of $\approx 2\text{ eV}$ ($\approx 1\text{ eV}$) for the smaller system, signifying the importance of the many-body corrections to LDA. The self-consistent iterations, labeled as G_nW_0 $n = 1, 2, \dots$, further decrease the VBM by as much as 0.34 eV and increase the CBM by 0.1 eV (for the smaller system). This leads to an increase in the predicted band gap by as much as 0.45 eV , correcting the tendency of G_0W_0 to underestimate ionization potentials.^{51–53} Our results show that the self-consistent correction to G_0W_0 decreases with the system size, suggesting that self-consistency leads to a small correction of the G_0W_0 in the bulk limit, consistent with previous results.^{8,30,54}

One simplification made in the sgrGW approach, is that the shifts in energy ($\Delta_{n \leq n_{\text{Fermi}}} \approx \Delta_v$ and $\Delta_{n > n_{\text{Fermi}}} \approx \Delta_c$) are independent of the band index n . To test this assumption, we have calculated the QP energies for all occupied KS eigenvalues and for unoccupied KS eigenvalues near the CBM. The QP energies were then fitted to a quadratic formula:

$$\varepsilon_n^{\text{QP}} = a_2 (\varepsilon_n^{\text{KS}})^2 + a_1 \varepsilon_n^{\text{KS}} + a_0, \quad (10)$$

where, a_2 is the non-rigidity parameter. For both QDs the fit yields a nearly linear relation for the occupied levels, with $a_2 = 0.01\text{ eV}^{-1}$, $a_1 = 1.22$ and $a_0 = -1.13\text{ eV}$ for $\text{Si}_{35}\text{H}_{36}$ and $a_2 = 0.00\text{ eV}^{-1}$, $a_1 = 0.96$, and $a_0 = -1.52\text{ eV}$ for $\text{Si}_{705}\text{H}_{300}$. A similar picture emerges for the unoccupied energies close to the CBM. This indicates a nearly constant QP shift for all states, consistent with the above simplification. This is also inline with the fact that LDA provides a good estimate of the band structure near the top of the valence and the bottom of the conduction bands, with a constant shift for both bands in the bulk limit.⁵⁵

B. Phosphorene nanoribbons

The sgrGW method is not limited to describe QP energies in systems confined in 3D and 2D materials. To illustrate this we apply the approach to study QPs in phosphorene nanoribbons (PNRs), focusing on planar and bent configurations (see the left panel of Fig. 2). Previous DFT based studies^{44–48} showed a sensitivity of charge localization and band gap on bending of 2D material. These effects, however, were not addressed at the level of many-body perturbation theory due to computational limitations resulting from the large system size.

We have performed sgrGW calculations of PNRs of dimensions 0.87 nm wide and 5.3 nm long. The system geometry was obtained from the experimental structure of

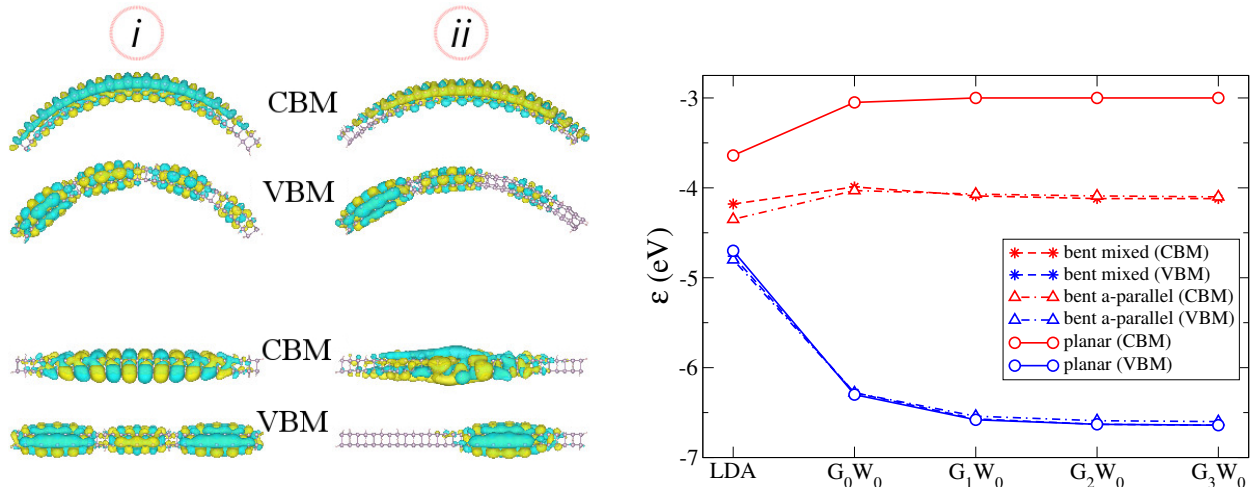


Figure 2. Left: CBM and VBM wave functions (positive and negative regions are shown by yellow and aqua color) are depicted for the bent and planar PNRs, using anti-parallel (*i*) and mixed (*ii*) hydrogen passivation schemes (see text). Right: The CBM and VBM QP energies for planar and bent configurations (using mixed and antiparallel passivation schemes). The LDA starting point of the calculation is also shown for reference. The different partially self-consistent sGW iterations are labeled $G_0W_0 \dots G_3W_0$.

black phosphorous.⁵⁶ The stressed PNRs were obtained by bending the system along the longer direction with a radius corresponding to 2.65 nm. The dangling bonds at the edges of the PNRs were passivated with hydrogen atoms. We consider three cases: Hydrogen atoms pointing in the same direction (parallel), pointing in an opposite direction (anti-parallel), or a mixed arrangement. While the ordered configurations (parallel or anti-parallel) are energetically favored over the mixed case, phosphorene is prone to rearrangements at the edges⁵⁷ and therefore, we consider all three passivation cases.

Both DFT and sgrGW employ a real-space grid with dimensions $192 \times 82 \times 100$ and spacing $h = 0.55a_0$ for the planar PNR, and $176 \times 64 \times 56$ with $h = 0.6a_0$ for the bent PNR. The LDA density, VBM and CBM were used as inputs for the sgrGW calculations with $N_\zeta = 1500$, and $N_\xi = 100$ and $N_\eta = 8$ for both systems. The time-grid and regularization parameters were identical to those used for the silicon QDs.

We first discuss the KS-DFT results for the VBM and CBM. The hypersurface of the corresponding QP wave functions, obtained from the DFT calculation, are shown in the left panel of Fig. 2. For the planar geometry the electron and hole densities are delocalized for the anti-parallel passivation while for the mixed (and parallel, not shown) passivation, we observe a localization which is stronger for the hole. For the bent structure, the effect of localization is less pronounced.

The QP energies shown in the right panel of Fig. 2 tell a different story. First, it is clear that the band gap increases significantly, by many folds, when many-body perturbation corrections are included. The VBM decreases by nearly ≈ 2 eV for G_0W_0 compared to the DFT result and the CBM increases by ≈ 0.75 eV. This

leads to an opening of the band gap by nearly a factor of 3, from 1.06 eV to 3.25 eV. The self consistent iterations further increase the gap to 3.64 eV mainly correcting the QP energy of the hole. This is also evident in the lower panel of Fig. 3 where $\varepsilon_n^{KS} + \tilde{\Sigma}_n(\omega) - V_{xc}^n$ is plotted versus ω for the single shot and sGW and the converged sgrGW. The QP energy Eq. (4) is given by the intersect with the straight line, for which $\varepsilon_n^{KS} + \tilde{\Sigma}_n(\omega) - V_{xc}^n = \omega$. For the hole, there is a marked effect of the self-consistent solution, where the intersect occurs at lower energies while for the electrons this is not case and the self-consistent solution is only slightly above the single-shot result.

For the bent configuration, we observe that the hole energy is largely insensitive to the bending and to the passivation, with the same effects of many-body perturbation theory on its energy as described above. The electron energy drops significantly upon bending but is sensitive to passivation only in DFT. Further, we find that the electron energy decreases slightly with the self consistent iterations unlike the situation for the planar geometry or for the silicon QDs. This effects is also evident in the upper panel of Fig. 3 where for both the hole and the electron the solid line (representing the self consistent function) appears below the dashed line (representing the single-shot results), signaling a decrease of the QP energy by imposing the partial self-consistency.

IV. SUMMARY AND CONCLUSIONS

A partially self-consistent band-gap renormalization GW approach was introduced and applied using the stochastic GW⁴¹ to large silicon QDs and phosphorene

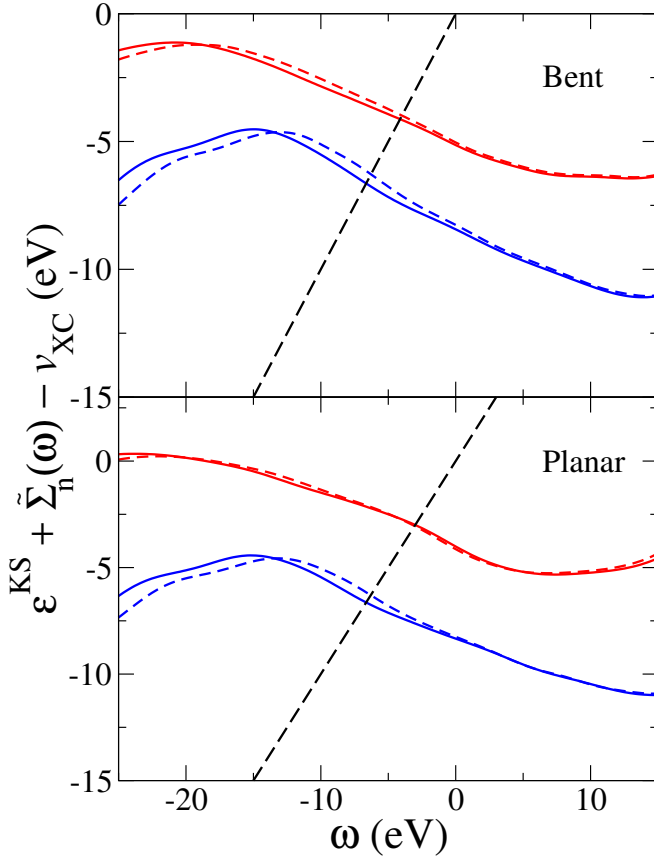


Figure 3. Graphical location of the QP particle energy for bent (top panel) and planar (bottom panel) PNRs. The QP energy is the frequency ω for which the straight-dashed-black line intersects the VBM (blue) and CBM (red) curves representing the right-hand side of the Eq. (4). The dashed and solid lines correspond to the G_0W_0 and G_4W_0 calculations, respectively.

nanoribbons for planar and bent geometries. The combined methodology (dubbed sgrGW) was used to show that the self-consistent iterations serve to open the gap further than single-shot GW. This opening can be as large as 10% compared to G_0W_0 . The self-consistent iterations were applied to a single-shot calculation as a post-processing step, i.e. after the completing the computationally intensive step of calculating the orbital-dependent self-energy, $\Sigma_n(t)$. The method can therefore be used to renormalize band-gaps of any GW method, which like stochastic GW produces $\Sigma_n(t)$ or the Fourier transformed $\tilde{\Sigma}_n(\omega)$ for all frequencies in the relevant frequency range. The band-gap renormalization GW method is expected to benefit systems for which the main GW corrections are in the fundamental band-gap renormalization and less so in the shape of the occupied and unoccupied bands.

ACKNOWLEDGMENTS

E.R. and D.N. acknowledge support by the NSF, Grants CHE-1465064 and DMR/BSF-1611382. R.B. acknowledges the US-Israel Binational Science foundation support under the BSF-NSF program, Grant 2015687. Part of the calculations were performed as part of the XSEDE computational project TG-CHE160092.⁵⁸

Appendix A: Stochastic pGW implementation

The stochastic formulation for the partially self-consistent GW described in the previous sections is based on the stochastic GW approach, developed in Ref. 41 and summarized in Ref. 42. The core idea is the use of a stochastic trace formula⁵⁹

$$\text{tr} \left\{ \hat{O}(t) \right\} \approx \frac{1}{N_\zeta} \sum_{\zeta} \left\langle \zeta | \hat{O}(t) | \zeta \right\rangle \equiv \left\langle \zeta | \hat{O}(t) | \zeta \right\rangle_{\zeta} \quad (\text{A1})$$

where $\zeta(\mathbf{r}) = \pm \frac{1}{h^{3/2}}$ is a real stochastic orbital, h^3 is the volume element, and N_ζ is the number of stochastic orbitals used to estimate the trace. The procedure is based on the following steps:

1. Choose a KS orbital, $\phi_n^{KS}(\mathbf{r})$, with a corresponding eigenvalue, ϵ_n^{KS} .
2. Take N_ζ stochastic orbitals $\zeta(\mathbf{r})$ and for each, take N_ξ stochastic orbitals $\xi(\mathbf{r})$.
3. Generate $A_{n\zeta\xi}(t) = \int \phi_n^{KS}(\mathbf{r}) \zeta(\mathbf{r}, t)^* \xi(\mathbf{r}) d\mathbf{r}$, where $\zeta(\mathbf{r}, t) = e^{-i\hat{h}_{KS}t/\hbar} \left[\theta(t) - \theta_\beta(\mu - \hat{h}_{KS}) \right] \zeta(\mathbf{r})$ is obtained by expanding $e^{-i\hat{h}_{KS}t/\hbar} \left[\theta(t) - \theta_\beta(\mu - \hat{h}_{KS}) \right]$ in a Chebyshev series.⁶⁰ Here, $\theta(t)$ is the Heaviside function, and $\theta_\beta(\epsilon) = \frac{1}{2} [1 + \text{erf}(\beta\epsilon)]$ (in the limit $\beta \rightarrow \infty$, $\theta_\beta(\epsilon) \rightarrow \theta(\beta\epsilon)$).
4. Generate $B_{n\zeta\xi}^r(t) = \iint \xi(\mathbf{r}) u_C(|\mathbf{r} - \mathbf{r}'|) \Delta n_{n\zeta}^r(\mathbf{r}', t) d\mathbf{r} d\mathbf{r}'$, where $\Delta n_{n\zeta}^r(\mathbf{r}, t) = \frac{1}{\tau} \left\langle |\eta_\tau(\mathbf{r}, t)|^2 - |\eta_{\tau=0}(\mathbf{r}, t)|^2 \right\rangle_\eta$. To obtain $\Delta n_{n\zeta}^r(\mathbf{r}, t)$, generate N_η independent stochastic orbitals $\eta(\mathbf{r})$. Perturb these orbitals with $\eta_\tau(\mathbf{r}, 0) = e^{-iv_{n\zeta}(\mathbf{r})\tau} \theta_\beta(\mu - \hat{h}_{KS}) \eta(\mathbf{r})$ and $\eta_{\tau=0}(\mathbf{r}, 0) = \theta_\beta(\mu - \hat{h}_{KS}) \eta(\mathbf{r})$, where $v_{n\zeta}(\mathbf{r}) = \int u_C(|\mathbf{r} - \mathbf{r}'|) \phi_n^{KS}(\mathbf{r}') \zeta(\mathbf{r}') d\mathbf{r}'$ is obtained using Fast Fourier Transform (FFT) for a convolution integral. Here, $u_C(r) = \frac{e^2}{4\pi\epsilon_0 r}$ is the bare Coulomb potential energy. Then, propagate these using the time-dependent Hartree equations: $i \frac{\partial}{\partial t} \eta_\tau(\mathbf{r}, t) = \hat{h}_{KS} \eta_\tau(\mathbf{r}, t) + \left(\int \frac{\Delta n_{n\zeta}^r(\mathbf{r}', t)}{|\mathbf{r} - \mathbf{r}'|} d\mathbf{r}' \right) \eta_\tau(\mathbf{r}, t)$ to generate $\Delta n_{n\zeta}^r(\mathbf{r}, t)$.

5. Fourier transform $B_{n\zeta\xi}^r(t) \rightarrow \tilde{B}_{n\zeta\xi}^r(\omega)$ and convert to the time-ordered quantity $\tilde{B}_{n\zeta\xi}^r(\omega)$ using⁶¹ $\tilde{B}_{n\zeta\xi}^r(\omega) = \text{Re}\tilde{B}_{n\zeta\xi}^r(\omega) + i \text{sign}(\omega) \text{Im}\tilde{B}_{n\zeta\xi}^r(\omega)$. Fourier transform back $\tilde{B}_{n\zeta\xi}^r(\omega) \rightarrow B_{n\zeta\xi}^r(t)$.
6. By averaging over ζ and ξ , calculate the self-energy $\Sigma_n^{(0)}(t) = \langle A_{n\zeta\xi}(t) B_{n\zeta\xi}(t) \rangle_{\zeta\xi} + \Sigma_n^X \delta(t)$. Here, $\Sigma_n^X = - \left\langle \int \phi_n^{KS}(\mathbf{r}) \zeta(\mathbf{r}, 0^-) v_\zeta^{\text{aux}}(\mathbf{r}) d\mathbf{r} \right\rangle_\zeta$, where $\zeta(\mathbf{r}, 0^-) = \theta_\beta \left(\mu - \hat{h}_{KS} \right) \zeta(\mathbf{r})$ is the (negative) $t = 0$ of $\zeta(\mathbf{r}, t)$ generated in step 3, and $v_\zeta^{\text{aux}}(\mathbf{r}) = \int u_C(|\mathbf{r} - \mathbf{r}'|) \zeta(\mathbf{r}') \phi_n^{KS}(\mathbf{r}') d\mathbf{r}'$ is obtained using FFT for a convolution integral.
7. Generate $\Sigma_n(t) = \Sigma_n^{(0)}(t) e^{-i\Delta(t)t}$ where $\Delta(t) =$

$\Delta_v \theta(-t) + \Delta_c \theta(t)$ and use the Fourier transform to generate $\tilde{\Sigma}_n(\omega) = \int_{-\infty}^{\infty} \Sigma_n(t) e^{i\omega t} dt$.

8. Solve Eq. (4) for ε_n^{QP} and obtain $\Delta_n = \varepsilon_n^{QP} - \varepsilon_n^{KS}$ for the VBM (Δ_v) and CBM (Δ_c) orbitals.

In sGW, steps 7 and 8 are performed only once with $\Delta(t) = 0$. In the sgrGW, steps 7 and 8 become part of the self consistent band gap renormalization described in the end of Section II, repeated until convergence of Eq. (4) is achieved for a predefined tolerance. Thus, the demanding portions of the stochastic GW are only performed once (steps 1-6) and self-consistency is performed as a post-processing step. This implies that the scaling of the sgrGW approach is identical to that of the sGW, which is nearly linear with the system size and the additional self-consistent iterations add a negligible amount of computational work.

-
- * vojtech@chem.ucla.edu
† roi.baer@huji.ac.il
‡ eran.rabani@berkeley.edu
§ dxn@chem.ucla.edu
- ¹ L. Hedin, Phys. Rev. **139**, A796 (1965).
 - ² F. Aryasetiawan and O. Gunnarsson, Rep. Prog. Phys. **61**, 237 (1998).
 - ³ M. M. Rieger, L. Steinbeck, I. White, H. Rojas, and R. Godby, Comput. Phys. Commun. **117**, 211 (1999).
 - ⁴ L. Steinbeck, A. Rubio, L. Reining, M. Torrent, I. White, and R. Godby, Comput. Phys. Commun. **125**, 05 (1999).
 - ⁵ G. Onida, L. Reining, and A. Rubio, Rev. Mod. Phys. **74**, 601 (2002).
 - ⁶ A. Rubio and S. G. Louie, "Quasiparticle AND optical properties of solids AND nanostructures: The gw-bse approach," in *Handbook of materials modeling*, edited by S. Yip (Springer, Dordrecht ; New York, 2005) p. 215.
 - ⁷ C. Friedrich and A. Schindlmayr, NIC Series **31**, 335 (2006).
 - ⁸ M. Shishkin and G. Kresse, Phys. Rev. B **75**, 235102 (2007).
 - ⁹ P. E. Trevisanutto, C. Giorgetti, L. Reining, M. Ladisa, and V. Olevano, Phys. Rev. Lett. **101**, 226405 (2008).
 - ¹⁰ C. Rostgaard, K. W. Jacobsen, and K. S. Thygesen, Phys. Rev. B **81**, 085103 (2010).
 - ¹¹ I. Tamblyn, P. Darancet, S. Y. Quek, S. A. Bonev, and J. B. Neaton, Phys. Rev. B **84**, 201402 (2011).
 - ¹² M. van Setten, F. Weigend, and F. Evers, J. Chem. Theory Comput. **9**, 232 (2012).
 - ¹³ G. Stefanucci and R. van Leeuwen, *Nonequilibrium Many-Body Theory of Quantum Systems: A Modern Introduction* (Cambridge University Press, 2013).
 - ¹⁴ M. Govoni and G. Galli, Journal of chemical theory and computation **11**, 2680 (2015).
 - ¹⁵ F. Kaplan, M. E. Harding, C. Seiler, F. Weigend, F. Evers, and M. J. van Setten, J. Chem. Theory Comput. (2016).
 - ¹⁶ W. Kohn and L. J. Sham, Phys. Rev. **140**, A1133 (1965).
 - ¹⁷ P. Hohenberg and W. Kohn, Phys. Rev. **136**, B864 (1964).
 - ¹⁸ J. Deslippe, G. Samsonidze, D. A. Strubbe, M. Jain, M. L. Cohen, and S. G. Louie, Comput. Phys. Commun. **183**, 1269 (2012).
 - ¹⁹ H.-V. Nguyen, T. A. Pham, D. Rocca, and G. Galli, Phys. Rev. B **85**, 081101 (2012).
 - ²⁰ M. S. Hybertsen and S. G. Louie, Phys. Rev. Lett. **55**, 1418 (1985).
 - ²¹ M. S. Hybertsen and S. G. Louie, Phys. Rev. B **34**, 5390 (1986).
 - ²² S. V. Faleev, M. Van Schilfgaarde, and T. Kotani, Phys. Rev. Lett. **93**, 126406 (2004).
 - ²³ F. Caruso, P. Rinke, X. Ren, M. Scheffler, and A. Rubio, Phys. Rev. B **86**, 081102 (2012).
 - ²⁴ F. Bruneval and M. A. Marques, J. Chem. Theory Comput. **9**, 324 (2012).
 - ²⁵ F. Bruneval, The Journal of chemical physics **136**, 194107 (2012).
 - ²⁶ M. J. van Setten, F. Caruso, S. Sharifzadeh, X. Ren, M. Scheffler, F. Liu, J. Lischner, L. Lin, J. R. Deslippe, S. G. Louie, C. Yang, F. Weigend, J. B. Neaton, F. Evers, and P. Rinke, J. Chem. Theory Comput. **11**, 5665 (2015).
 - ²⁷ J. W. Knight, X. Wang, L. Gallandi, O. Dolgounitcheva, X. Ren, J. V. Ortiz, P. Rinke, T. Körzdörfer, and N. Marom, J. Chem. Theory Comput. (2016).
 - ²⁸ A. Stan, N. E. Dahlen, and R. Van Leeuwen, J. Chem. Phys. **130**, 114105 (2009).
 - ²⁹ X. Blase and C. Attaccalite, Appl. Phys. Lett. **99**, 171909 (2011).
 - ³⁰ F. Bruneval and M. Gatti, in *First Principles Approaches to Spectroscopic Properties of Complex Materials* (Springer, 2014) pp. 99–135.
 - ³¹ J. E. Northrup, M. S. Hybertsen, and S. G. Louie, Physical review letters **59**, 819 (1987).
 - ³² D. Neuhauser, E. Rabani, and R. Baer, J. Chem. Theory Comput. **9**, 24 (2013).
 - ³³ R. Baer and E. Rabani, Nano Lett. **12**, 2123 (2012).
 - ³⁴ D. Neuhauser, E. Rabani, and R. Baer, J. Phys. Chem. Lett. **4**, 1172 (2013).
 - ³⁵ R. Baer, D. Neuhauser, and E. Rabani, Phys. Rev. Lett. **111**, 106402 (2013).
 - ³⁶ Q. Ge, Y. Gao, R. Baer, E. Rabani, and D. Neuhauser, J. Phys. Chem. Lett. **5**, 185 (2013).

- ³⁷ D. Neuhauser, R. Baer, and E. Rabani, *J. Chem. Phys.* **141**, 041102 (2014).
- ³⁸ Y. Gao, D. Neuhauser, R. Baer, and E. Rabani, *J. Chem. Phys.* **142**, 034106 (2015).
- ³⁹ E. Rabani, R. Baer, and D. Neuhauser, *Phys. Rev. B* **91**, 235302 (2015).
- ⁴⁰ D. Neuhauser, E. Rabani, Y. Cytter, and R. Baer, *J. Phys. Chem. A* **120**, 3071 (2015).
- ⁴¹ D. Neuhauser, Y. Gao, C. Arntsen, C. Karshenas, E. Rabani, and R. Baer, *Phys. Rev. Lett.* **113**, 076402 (2014).
- ⁴² V. Vlček, E. Rabani, D. Neuhauser, and R. Baer, *J. Chem. Theory Comput.* **submitted** (2016).
- ⁴³ V. Vlček, H. R. Eisenberg, G. Steinle-Neumann, E. Rabani, D. Neuhauser, and R. Baer, *Phys. Rev. Lett.* **116**, 186401 (2016).
- ⁴⁴ X. Peng, Q. Wei, and A. Copple, *Phys. Rev. B* **90**, 085402 (2014).
- ⁴⁵ A. Rodin, A. Carvalho, and A. Castro Neto, *Phys. Rev. Lett.* **112**, 176801 (2014).
- ⁴⁶ R. Fei and L. Yang, *Nano Lett.* **14**, 2884 (2014).
- ⁴⁷ L. Seixas, A. S. Rodin, A. Carvalho, and A. H. Castro Neto, *Phys. Rev. B* **91**, 115437 (2015).
- ⁴⁸ L. Yu, A. Ruzsinszky, and J. P. Perdew, *Nano letters* **16**, 2444 (2016).
- ⁴⁹ L. W. Wang and A. Zunger, *J. Phys. Chem.* **98**, 2158 (1994).
- ⁵⁰ N. Troullier and J. L. Martins, *Phys. Rev. B* **43**, 1993 (1991).
- ⁵¹ F. Caruso, P. Rinke, X. Ren, M. Scheffler, and A. Rubio, *Phys. Rev. B* **86**, 081102 (2012).
- ⁵² M. J. van Setten, F. Caruso, S. Sharifzadeh, X. Ren, M. Scheffler, F. Liu, J. Lischner, L. Lin, J. R. Deslippe, S. G. Louie, *et al.*, *J Chem Theory Comput* **11**, 5665 (2015).
- ⁵³ J. W. Knight, X. Wang, L. Gallandi, O. Dolgounitcheva, X. Ren, J. V. Ortiz, P. Rinke, T. Körzdörfer, and N. Marom, *J. Chem. Theory Comput.* **12**, 615 (2016).
- ⁵⁴ L. Hedin, *J. Phys.: Condens. Matter* **11**, R489 (1999).
- ⁵⁵ R. W. Godby, M. Schlüter, and L. J. Sham, *Phys. Rev. Lett.* **56**, 2415 (1986).
- ⁵⁶ L. Cartz, S. R. Srinivasa, R. J. Riedner, J. D. Jorgensen, and T. G. Worlton, *J. Chem. Phys.* **71**, 1718 (1979).
- ⁵⁷ L. Liang, J. Wang, W. Lin, B. G. Sumpter, V. Meunier, and M. Pan, *Nano letters* **14**, 6400 (2014).
- ⁵⁸ J. Towns, T. Cockerill, M. Dahan, I. Foster, K. Gaither, A. Grimshaw, V. Hazlewood, S. Lathrop, D. Lifka, G. D. Peterson, *et al.*, *Computing in Science & Engineering* **16**, 62 (2014).
- ⁵⁹ M. F. Hutchinson, *Communications in Statistics-Simulation and Computation* **19**, 433 (1990).
- ⁶⁰ R. Kosloff, *J. Phys. Chem.* **92**, 2087 (1988).
- ⁶¹ A. L. Fetter and J. D. Walecka, *Quantum Theory of Many Particle Systems* (McGraw-Hill, New York, 1971) p. 299.